Available online at www.sciencedirect.com
ScienceDirect
Tectonophysics 426 (2006) 153–166
TECTONOPHYSICS
www.elsevier.com/locate/tecto

The Gibraltar Arc seismogenic zone (part 2): Constraints on a shallow east dipping fault plane source for the 1755 Lisbon earthquake provided by tsunami modeling and seismic intensity

M.-A. Gutscher [a,*], M.A. Baptista [b], J.M. Miranda [b]

[a] *IUEM, Univ. Brest, UMR 6538, Plouzané, France*
[b] *Inst. of Geophysics, Univ. Lisbon, Portugal*

Accepted 7 February 2006
Available online 7 July 2006

Abstract

The Great Lisbon earthquake has the largest documented felt area of any shallow earthquake and an estimated magnitude of 8.5–9.0. The associated tsunami ravaged the coast of SW Portugal and the Gulf of Cadiz, with run-up heights reported to have reached 5–15 m. While several source regions offshore SW Portugal have been proposed (e.g.— Gorringe Bank, Marquis de Pombal fault), no single source appears to be able to account for the great seismic moment as well as all the historical tsunami amplitude and travel time observations. A shallow east dipping fault plane beneath the Gulf of Cadiz associated with active subduction beneath Gibraltar, represents a candidate source for the Lisbon earthquake of 1755.

Here we consider the fault parameters implied by this hypothesis, with respect to total slip, seismic moment, and recurrence interval to test the viability of this source. The geometry of the seismogenic zone is obtained from deep crustal studies and can be represented by an east dipping fault plane with mean dimensions of 180 km (N–S) × 210 km (E–W). For 10 m of co-seismic slip an Mw 8.64 event results and for 20 m of slip an Mw 8.8 earthquake is generated. Thus, for convergence rates of about 1 cm/yr, an event of this magnitude could occur every 1000–2000 years. Available kinematic and sedimentological data are in general agreement with such a recurrence interval. Tsunami wave form modeling indicates a subduction source in the Gulf of Cadiz can partly satisfy the historical observations with respect to wave amplitudes and arrival times, though discrepancies remain for some stations. A macroseismic analysis is performed using site effect functions calculated from isoseismals observed during instrumentally recorded strong earthquakes in the region (M7.9 1969 and M6.8 1964). The resulting synthetic isoseismals for the 1755 event suggest a subduction source, possibly in combination with an additional source at the NW corner of the Gulf of Cadiz can satisfactorily explain the historically observed seismic intensities. Further studies are needed to sample the turbidites in the adjacent abyssal plains to better document the source region and more precisely calibrate the chronology of great earthquakes in this region.

Keywords: Great Lisbon earthquake; Iberia; Morocco; Subduction; Tsunami

1. Introduction

The Great Lisbon earthquake of 1755 with an estimated magnitude of 8.5–9.0 was felt as far away as Hamburg, the Azores and Cape Verde Islands and has

* Corresponding author. Tel.: +33 2 98 49 87 27; fax: +33 2 98 49 87 60.
E-mail address: gutscher@univ-brest.fr (M.-A. Gutscher).

0040-1951/$ - see front matter © 2006 Elsevier B.V. All rights reserved.
doi:10.1016/j.tecto.2006.02.025

the largest documented felt area of any shallow earthquake (Martinez-Solares et al., 1979; Johnston, 1996) (Fig. 1). The earthquake which struck on 1 November 1755 (All Saints Day) caused up to 100,000 deaths (Chester, 2001) through destruction by ground shaking, from the ensuing fires and by tsunami waves of 5–15 m which devastated the coasts of Southwest Iberia and Northwest Morocco (Baptista et al., 1998a). However, to this day the source of this great earthquake remains unknown (Gutscher, 2004).

While it is difficult to accurately determine the magnitude of great historical earthquakes like the 1755 event, comparison to recent strong earthquakes can be useful. The 1969 Cape St. Vincent earthquake with an instrumentally determined magnitude of Mw=7.9 provided such an opportunity (Fukao, 1973; Buforn et al., 1988). This event, which had a pure thrust type focal mechanism, was located in the Horseshoe abyssal plain (4700 m water depth) and generated a modest tsunami. The observed tsunami amplitudes at Cascais (near Lisbon), Lagos (near Cape St. Vincent) and Cadiz in 1969 were 50 cm, 50 cm and 10 cm respectively (Gjevik et al., 1997). For comparison, the historically reported tsunami wave heights for these same locations in 1755 were 6 m, >10 m and 15 m, respectively. This demonstrates the tremendous energy liberated by the 1755 event and implies that it was significantly stronger than the 1969 earthquake (Baptista et al., 1998a).

Previous studies of the 1755 earthquake have proposed prominent basement highs off the SW Iberia margin, such as the Gorringe Bank (Johnston, 1996) or the Marquis de Pombal (Zitellini et al., 2001; Gracia et al., 2003) to be the likely source (Fig. 1). Yet the relatively modest surface areas of these source regions

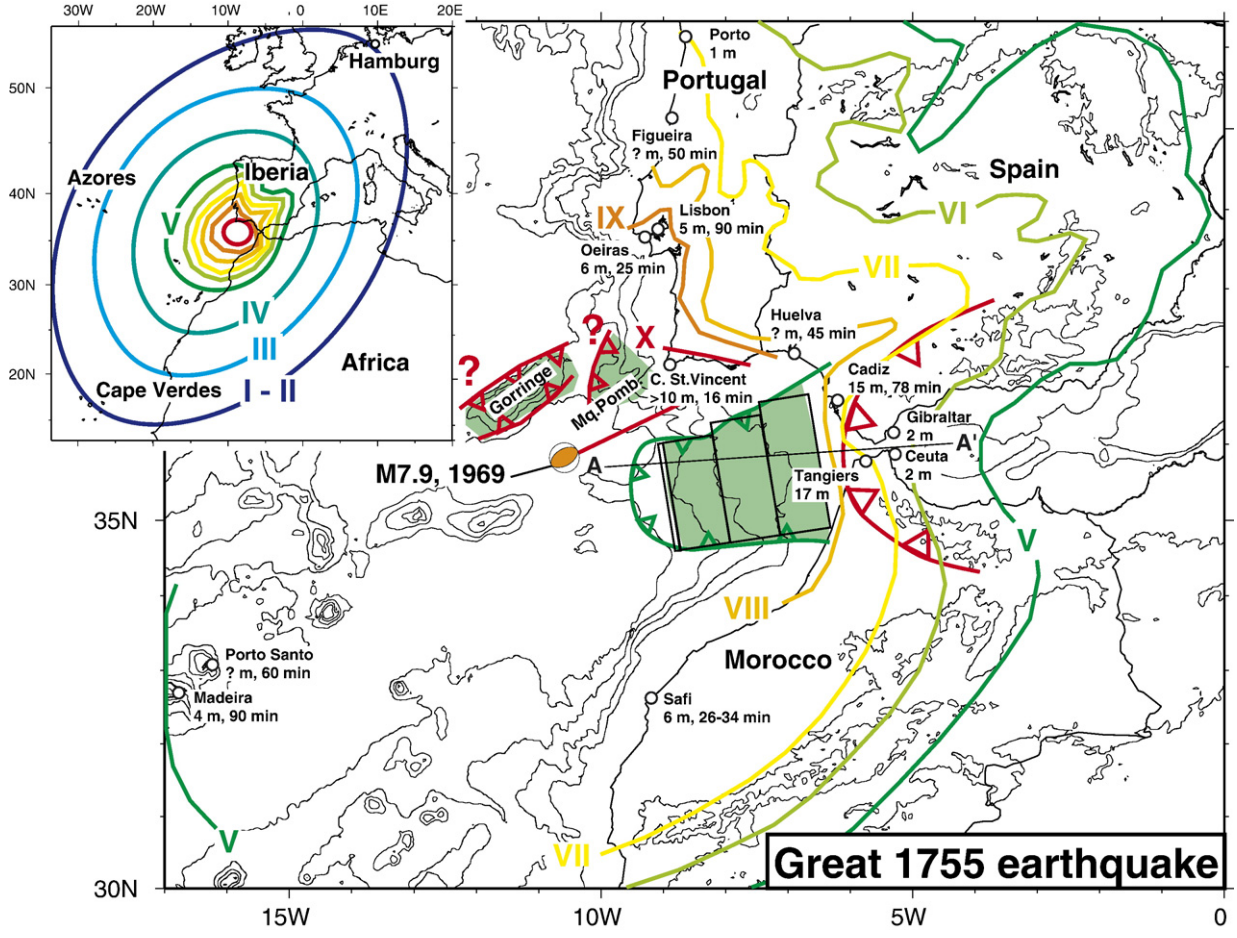

Fig. 1. Isoseismal map of the 1755 earthquake (after Martinez-Solares et al., 1979; Levret, 1991). Inset shows entire felt zone in NW Africa, western Europe and the NE Atlantic (after Johnston, 1996). Bathymetry shown as 1000 m contours (Sandwell and Smith, 1997). The 1969 Cape St. Vincent earthquake occurred on the N60E trending Horseshoe Fault. Historically reported tsunami arrival times and amplitudes are given for cities in the study area (Baptista et al., 1998a).

make it difficult to explain the seismic moment, for a reasonable set of fault parameters (e.g. — co-seismic displacement, rigidity, recurrence), consistent with the slow, NW–SE relative convergence between Africa and Iberia at about 4 mm/a (Argus et al., 1989; Fernandes et al., 2003). Seismic images of the crustal structure in the

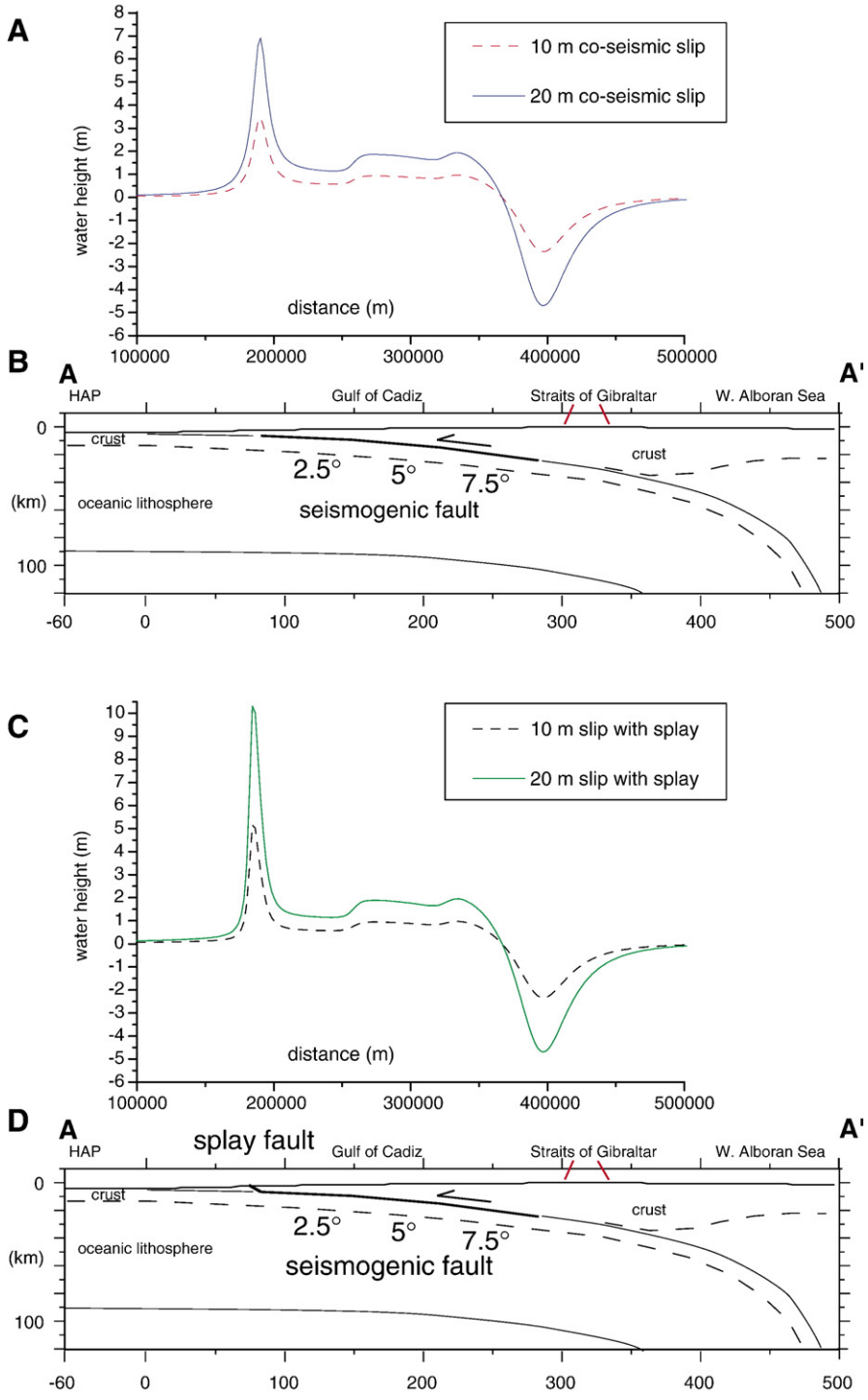

Fig. 2. Cross-section through the subduction fault plane (A–A′ in Fig. 1), showing the geometry of the sources tested (with and without fault splay) for different amounts of fault slip (10 and 20 m) and the initial seafloor displacement associated with each.

Gulf of Cadiz and tomographic images indicate an active accretionary wedge, overlying an eastward dipping basement and connected to a steep, east dipping slab of cold, oceanic lithosphere beneath Gibraltar (Gutscher et al., 2002).

In this paper, we use the geometry of the shallow east dipping fault plane of the Gibraltar subduction as determined in a parallel study (Thiebot and Gutscher, 2006-this volume) (Fig. 1) and calculate the ensuing seismic moment, as well as model synthetic tsunami waves generated by rupture along such a fault plane. Furthermore, we perform a macroseismic analysis, using a regional site effect function (derived here) and calculate synthetic isoseismals for a subduction source in addition to other possible sources and compare these to isoseismal maps based on historical observations. Finally, we consider the recurrence time for great earthquakes along this subduction plane in terms of sedimentological observations and regional kinematic data.

2. Subduction plane fault parameters

Deep seismic reflection and refraction profiles image an east dipping decollement and east dipping basement linked to the subduction zone beneath Gibraltar. Numerical modeling of the temperature distribution along the subduction interface suggests a seismogenic zone with a downdip width of about 200 km (Thiebot and Gutscher, 2006-this volume). These geometric parameters were used as a starting point for the earthquake source. We represent the principal fault plane using a series of rectangular sub-planes extending from 6.5 km depth eastwards to a maximum depth of 24 km (Fig. 2, Table 1). The dip increases progressively from 2.5°, to 5° to 7.5°. We also test a model with a frontal fault splay, extending from the seafloor to 6.5 km depth, where it joins the principal fault plane (Fig. 2). Fault splays within an accretionary wedge are considered to be potentially active during co-seismic slip and may contribute to the generation of tsunamis (Park et al., 2002; Satake et al., 2003). Moment magnitudes are calculated here for two different uniform co-seismic slips of 20 and 10 m. The mean dimensions of the fault plane are:

$$\begin{aligned} &\mathrm{N-S\ length} = 180\ \mathrm{km},\\ &\mathrm{total}\quad \mathrm{E-W\ width} = 210\ \mathrm{km}, \end{aligned}$$

Seismic moment is calculated according to the equation:

$$\begin{aligned} &\mathrm{Mo} = \mu \mathrm{SD},\ \mu = 3\times 10^{10}\mathrm{Pa}\\ &\text{rupture area } \mathrm{S} = 37800\ \mathrm{km}^2,\\ &\text{for slip of } \mathrm{D} = 20\ \mathrm{m}\\ &\mathrm{Mo} = 2.27\times 10^{22}\mathrm{Nm}\\ &\mathrm{Mw} = 2/3\log\ \mathrm{Mo}-6.03,\ \text{yields } \mathrm{Mw} = 8.80 \end{aligned}$$

$$\begin{aligned} &\text{for a slip } \mathrm{D} = 10\ \mathrm{m}\\ &\mathrm{Mo} = 1.13\times 10^{22}\ \mathrm{Nm}\\ &\text{yields } \mathrm{Mw} = 8.64 \end{aligned}$$

For comparison, the Great Alaska earthquake of 1964 had a rupture area of

$$750\ \mathrm{km}\times 200\ \mathrm{km}\ \text{and a mean slip } \mathrm{D} = 10\ \mathrm{m}.$$
$$\text{Thus, } \mathrm{Mo}=4.5\times 10^{22}\ \mathrm{Nm} \text{ and } \mathrm{Mw}=9.1.$$

For the 1964 Alaska earthquake, however, two major asperities ruptured and were calculated (on the basis of geodetic and tsunami inversions) to have slips reaching 10–15 m and 20–25 m (Holdahl and Sauber, 1994; Johnson et al., 1996). The rupture of 1755, may likewise have had a mean slip of 10 m, but with local peak displacements up to 20 m.

3. Tsunami modeling

The above simplified, fault plane was used to perform tsunami wave form modeling of a shallow east dipping subduction source. The initial displacement of the seafloor, that we consider to be similar to the initial displacement of the water surface, is calculated using the elastic half-space approach (Okada, 1985). The vertical displacement (for a pure thrust mechanism) is shown

Table 1
Source parameters of rectangular fault plane segments (given in UTM29 coordinates in m)

Segment	Dip	South		Nord		Degrees		m		
		X seg	*Y* seg	*X* seg	*Y* seg	Strike	Rake	Slip	Width	Length
Splay	30	516047	3825131	485098	3984165	−11,0125	90	10/20	6000	162017
Plane 1	2.5	521937	3826277	490988	3985311	−11,0125	90	10/20	68258	162017
Plane 2	5.0	588938	3839316	557989	3998350	−11,0125	90	10/20	68065	174017
Plane 3	7.5	655750	3852318	624801	4011352	−11,0125	90	10/20	68065	198017

Note the dip of the fault plane increases towards the east, with increasing depth (see Fig. 2).

along a profile perpendicular to the fault plane for the 4 cases tested, 10 m and 20 m slip, without and with a splay fault (Fig. 2A–D). Initial seafloor displacement is least for 10 m slip and no splay fault, with a maximum of + 3.5 m and a minimum of −2.4 m. The greatest seafloor displacement is obtained for the case with 20 m slip, including the splay fault, and ranges from +10 m at the western end of the Gulf of Cadiz to −5 m at the eastern end. This initial sea-surface displacement then propagates throughout the Atlantic in the Iberia — NW Africa region (Fig. 3). For a tsunami wave in deep water, the propagation velocity is approximately proportional to the square root of the water depth $v=(gh)^{1/2}$. Across regions at 4000 m water depth for instance, the tsunami wave travels at a velocity of 720 km/h (approximately the speed of a jet airplane). For a water depth of 1000 m, the velocity drops to 360 km/h and so on. The velocity of wave propagation drops dramatically, when shallow continental shelf regions are encountered. Thus, a good regional bathymetric model is required for accurately modeling tsunami arrival times. Here we use the global 2 min bathymetric grid (Smith and Sandwell, 1997), obtained by combining satellite altimetry with available depth soundings along ship tracks. Finite difference software SWAN Code (Mader, 1988) was applied to calculate wave propagation, using a shallow water non-linear wave model and a cell size of 0.025°. The regional propagation of the tsunami wave is illustrated at map scale in three time steps (Fig. 3).

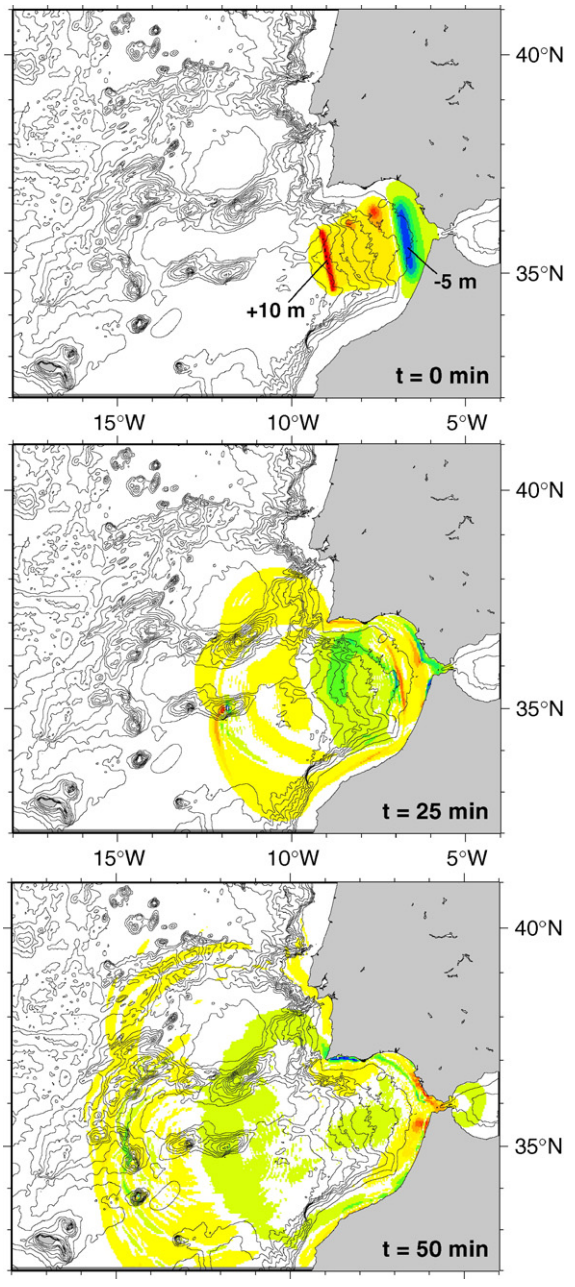

Fig. 3. Three-part time sequence showing propagation of tsunami wave in map view. At time zero, the initial displacement of the seafloor, corresponding to the initial displacement of the surface of the sea, is shown. Bathymetry as in Fig. 1.

Synthetic mareograms were calculated for over a dozen stations in the SW Iberia, NW African region (Fig. 4). These stations were selected for the most part on the availability of historical records and in some cases to avoid non-linear propagation effects in shallow water estuaries, which may induce significant modeling errors. For instance, we did not model the travel time and wave heights for Lisbon, where propagation is deeply affected by the shallow Tagus Estuary, which cannot be adequately represented by our bathymetric model. Instead we considered Oeiras, a small town just west of Lisbon harbor, where we also have good historical information. Similarly when modeling travel times and wave heights in Huelva (Spain), we also considered the neighboring Portuguese city of Vila Real de San Antonio (which was severely damaged by the 1755 earthquake and tsunami and completely rebuilt similar to downtown Lisbon, but is not influenced by propagation in an estuary).

Synthetic mareograms provide information on wave phase as well as the period (duration) of a tsunami wave. There are contradictions between the different compilations of historical records on the polarity of the first wave at the SW Spanish coast. Martinez-Solares et al. (1979) report a withdrawal, while Baptista et al. (1998a) cite 1756 Spanish documents describing a flux from the sea. Our synthetic mareograms for Huelva and Cadiz show, respectively, a temporary drop in sea-level of 1.5, and 5 m, respectively, before the positive tsunami wave arrived (Fig. 4A). The mean period of the modeled

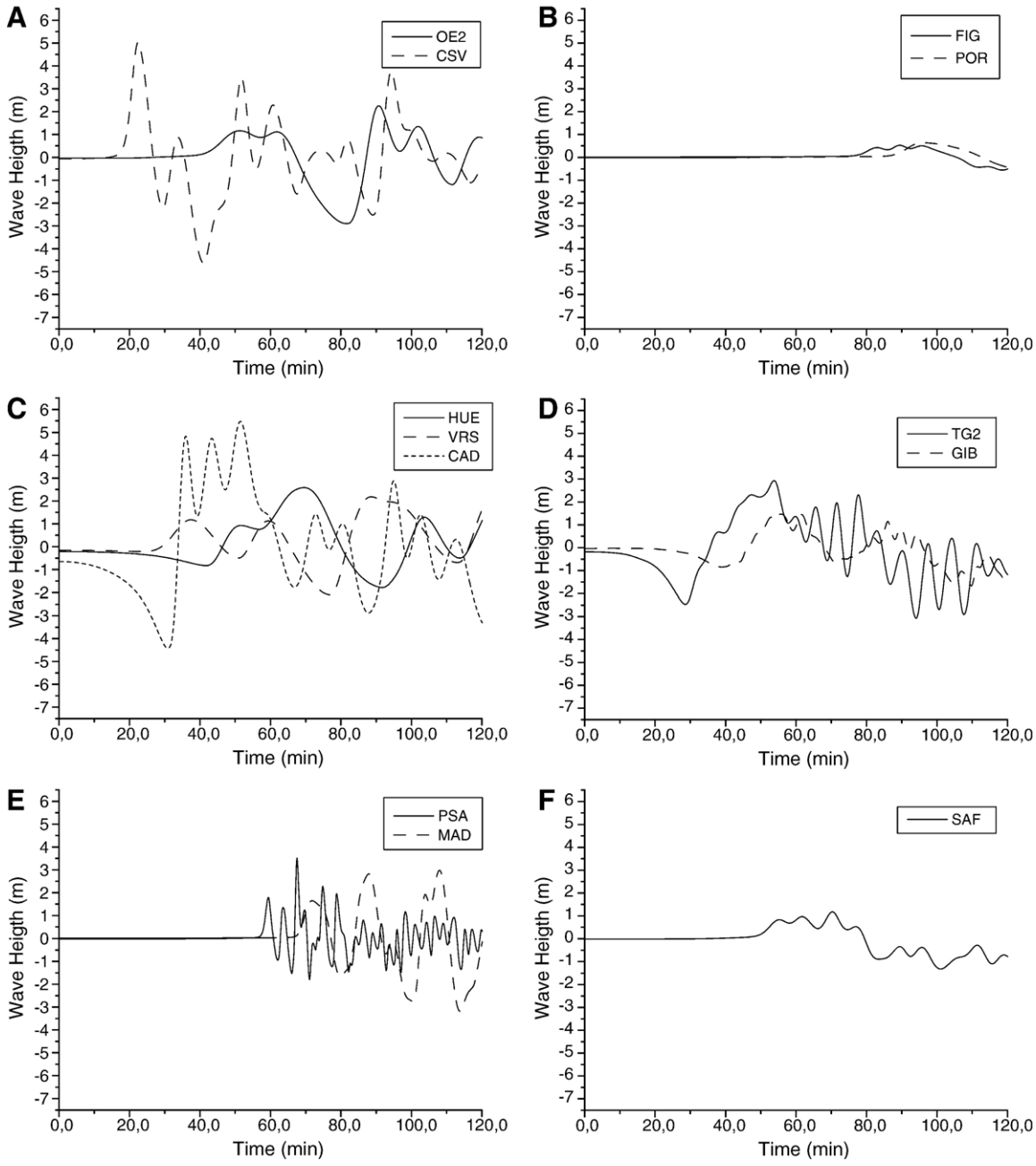

Fig. 4. Synthetic mareograms A) Portuguese west coast stations (south): Cape St. Vincent, Oeiras, B) Portuguese west coast stations (north): Figueira, Porto, C) Gulf of Cadiz stations: Huelva, Villa Real, Cadiz, D) Tangiers and Gibraltar, E) Madeira Island stations: Porto Santo, Madeira, F) Safi (western Morocco).

tsunami waves for the Cadiz station is about 20–40 min, which is in good agreement with historical reports (Baptista et al., 1998a).

Calculated travel times are compared to historical observations in Table 2. Modeled tsunami travel times show good agreement for the Cape St. Vincent (6 min difference) and Madeira stations (5-15 min difference). The modeled arrivals for Huelva and Villa Real are 7 min later and 8 min earlier, respectively, than the reported 45 min. The modeled arrival time for Cadiz is about 40 min too early (36 min vs. 78 min). This is a consequence of the eastward extent of the deep fault plane, where the down-dip limit was taken on the

Table 2
Comparison of historically observed tsunami arrival times with calculated arrival times from tsunami modeling of a shallow east dipping source and compared to calculated arrival times from a source at the Marquis de Pombal "source B" (N160) (Baptista et al., 1998b)

Station	Historical TT	Modelled TT	Marq. Pomb. TT
Cape St. Vincent	16 min	22 min	25 min
Huelva	45 min	52 min	80 min
Cadiz	78 min	36 min	70 min
Gibraltar	??	53 min	No TT
Tangiers	??	54 min	No TT
Porto Santo	60 min	59 min	68 min
Madeira	90 min	72 min	78 min
Safi (NW Morocco)	30 min	55 min	75 min
Oeiras	25 min	51 min	28 min
Lisbon	90 min	(not modelled, shallow water)	
Figueira	50 min	83 min	53 min
Porto	??	96 min	90 min

basis of thermal modelling of forearc thermal structure (Thiebot and Gutscher, 2006-this volume). A shorter "deep" fault plane would yield a larger travel time to Cadiz and provide a better travel time fit, while slightly reducing the total seismic moment. Arrival times for the Portuguese west coast and Safi, are about 25–40 min later than historical reports. This may be due to a combination of several possible causes: substantial delays due to poorly constrained shallow shelf bathymetry, inaccuracy of historical reports or multiple tsunami sources.

Calculated wave amplitudes are compared to historical observations in Table 3 for the four cases tested. Modeled tsunami amplitudes are greatest in the Gulf of Cadiz — Cape St. Vincent region, in agreement with historical observations. However, most modeled amplitudes are significantly less than historical reports (30–50% of the reported amplitudes for the 20 m fault splay source). An even greater discrepancy exists for Safi (Morocco) where only a 1.2 m high wave is modeled but a 6 m wave was reported. For many stations some of this discrepancy may be due to run-up effects, which have been estimated to locally increase tsunami amplitudes by 30% (Baptista et al., 1998b). But for Safi another explanation must be sought.

Given the systematically late arrivals and low amplitudes for the Portuguese west coast stations, it appears that the subduction source proposed here, cannot alone reproduce the observed tsunami for the entire region and that a contribution from an additional source further to the NW may be necessary. However, the subduction source is better able to account for the reported tsunami arrival times for the stations Huelva, Cape St. Vincent, Safi and Gibraltar than earlier models based on a single source on the Marquis de Pombal (Baptista et al., 1998b) (Table 2) and amplitudes are somewhat closer to historical reports for the stations Cadiz, Gibraltar, Madeira (Table 3).

4. Macroseismic analysis

Macroseismic analysis can be helpful in reconstructing sources for historical earthquakes where instrumental recordings are absent. The Iberia — NW African region, has been struck by strong earthquakes in the recent past, which can be used to establish a regional attenuation function (Levret, 1991; Johnston, 1996), as well as to determine local site effects. The two strongest recent events were the M7.9 St. Vincent earthquake of 1969 (Fukao, 1973) and an M6.5 event in the northern Gulf of Cadiz in 1964 (Udias and Arroyo, 1970) (Fig. 5). Once the site effects have been determined, synthetic isoseismal maps can be produced for hypothetical sources as demonstrated in similar studies (Mendes Victor et al., 1999; Baptista et al., 2003). Attenuation functions (of epicentral distance vs. intensity) have been proposed for the 1755 and 1969 earthquakes (Levret, 1991). Here, we subtract the radial attenuation functions (Fig. 6A,B) from published maps of seismic intensity and determine the local site effect for both the 1969 and the 1964 events (Fig. 6C,D). Although each particular ray path can locally influence the felt intensity, certain general patterns are reflected in both site effect maps. Next, we calculate a mean site effect map taking an average of the 1969 and 1964 site effect maps (Fig. 7). (N.B. — This averaging

Table 3
Comparison of historically observed tsunami wave amplitudes with calculated amplitudes from tsunami modeling of a shallow east dipping source and compared to calculated amplitudes from a source at the Marquis de Pombal (N160 source) (Baptista et al., 1998b)

Station	Historical amplitude	10 m	20 m	Modelled amplitude		Marq. Pomb.
				10 m (splay)	20 m (splay)	(20 m slip)
Cape St. Vincent	>10 m	2.2 m	4.4 m	2.5 m	5.0 m	6.0 m
Huelva	??	1.1 m	2.3 m	1.3 m	2.6 m	–
Cadiz	15 m	2.4 m	4.8 m	2.7 m	5.5 m	5.0 m
Gibraltar	2 m	0.7 m	1.3 m	1.4 m	1.4 m	4.5 m
Tangiers	(17 m ??)	1.4 m	2.8 m	1.4 m	2.9 m	–
Porto Santo	3 m	1.1 m	1.7 m	2.2 m	3.5 m	–
Madeira	4 m	1.4 m	1.5 m	2.7 m	3.0 m	<1.5 m
Safi (NW morocco)	6 m	0.5 m	0.6 m	1.1 m	1.2 m	2.0 m
Oeiras	6 m	1.1 m	1.1 m	2.2 m	2.2 m	10.0 m
Lisbon	5 m	(not modelled, shallow water)				–
Figueira	??	0.2 m	0.4 m	0.2 m	0.5 m	–
Porto	1 m	0.3 m	0.6 m	0.3 m	0.7 m	–

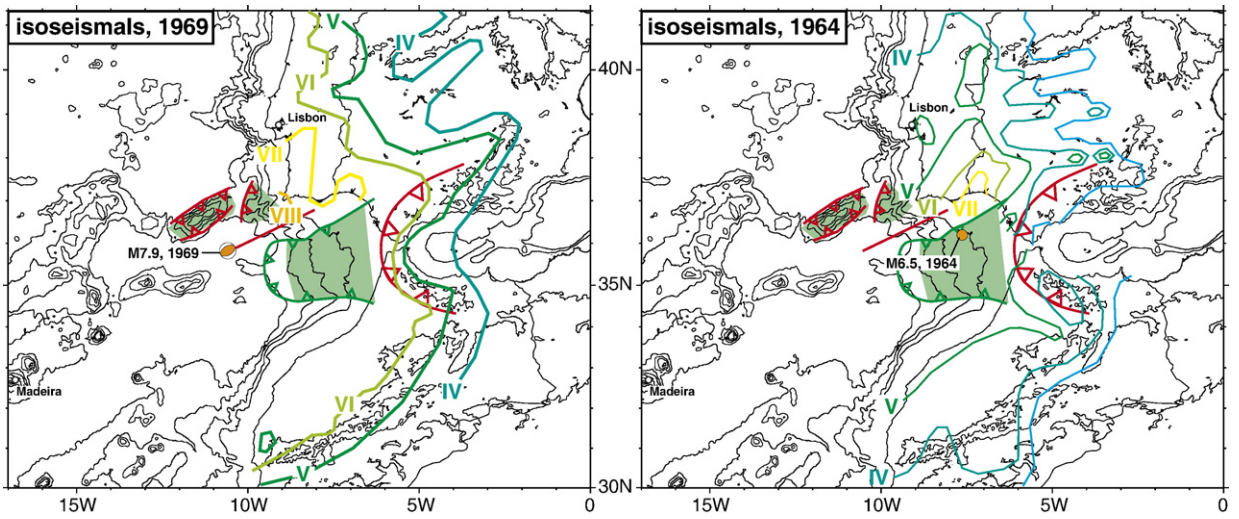

Fig. 5. Isoseismal maps a) M7.9 Cape St. Vincent earthquake of 1969, b) M6.8 Gulf of Cadiz earthquake of 1964. Bathymetry as in Fig. 1.

process results in 0.5 MSK intensity contours. While we recognize that such precision is not possible with respect to felt seismic intensity, one can consider the probability of the intensity at this site being the next highest full *I* value, or the next lowest full *I* value, to be 50%).

The averaged site effect map shows strong attenuation from the southern Portuguese coast (Algarve) towards the NE to the Variscan Massifs of Central Iberia. Strong attenuation is observed as well in the internal zones of the Betic–Rif orogen and the Western Alboran Sea. Conversely, there are moderate amplification effects in the Guadalquivir Basin (Betic foreland basin), and the Rharb Basin (Rif foreland basin). Finally, strong amplification is found in the Agadir Basin (SW Morocco) and in the Porto region of NW Portugal. In almost all cases the amplification is related to Cenozoic sedimentary basins, a correlation pointed out in a previous study (Levret, 1991). The regions of greatest attenuation commonly correlate with crystalline massifs, except for the thickly sedimented and thinned crustal domain of the West Alboran Sea. Here attenuation may be due to the low p-wave velocity and low Q anomaly in the upper mantle of the West Alboran domain (Calvert et al., 2000), caused by vigorous convection in the back-arc. Next, by taking a published regional attenuation function for the 1755 event (Levret, 1991) and adding our mean site function, we calculated synthetic isoseismals for the 1755 earthquake.

Three potential source regions were considered. In each case the source region (with constant intensity) has a radius of 100 km and beyond this distance intensity diminishes according to the radial attenuation function of Levret (1991). The first source centered at 8° W, 35.5° N corresponds to the subduction fault plane (Fig 8A). The resulting synthetic isoseismal map (Fig. 8B) predicts very high intensities in SW Spain and NW Morocco (*I*=8–9). While such intensities were reported for Cadiz and Sevilla, these values are 1–2 intensities higher than historical reports from Morocco. And the predicted intensity for Lisbon at 7.5 is about 1.5 too low. The second source centered at 8.5° W, 36° N (Fig. 8C) is at the NW edge of the subduction fault plane. This could represent either a large slip asperity along the fault plane in this vicinity, or alternatively, the combined moment release from the subduction fault plane and from a N75E oriented fault, representing the Africa–Eurasia plate boundary in the northern Gulf of Cadiz (Jimenez-Munt et al., 2001; Negredo et al., 2002) and situated at the northern edge of the accretionary wedge. Slip along this fault has been interpreted to be the source of the 1964 M6.5 earthquake in the Northern Gulf of Cadiz (Udias and Arroyo, 1970). The resulting synthetic isoseismal map (Fig. 8D), predicts *I*=10 along the Algarve coast, *I*=8–9 in SW Spain and *I*=8–9 in NW Morocco. Lisbon with a predicted intensity of 8 is also closer to the historically reported *I*=9. Thus, the overall fit is satisfactory. Finally, the third source is centered at 9.5° W, 36.5° N (Fig. 8E) about 100 km SW of Cape St. Vincent (SW tip of Portugal). This could represent the Marquis de Pombal together with an east trending segment of the Africa–Iberia plate boundary. The resulting synthetic isoseismal map (Fig. 8F) predicts *I*=10 at the SW corner of Portugal, *I*=8–9 in Lisbon and *I*=6–7 throughout NW Morocco. The overall fit to the historically reported isoseismals is very good in Iberia and satisfactory in Morocco. However, some uncer-

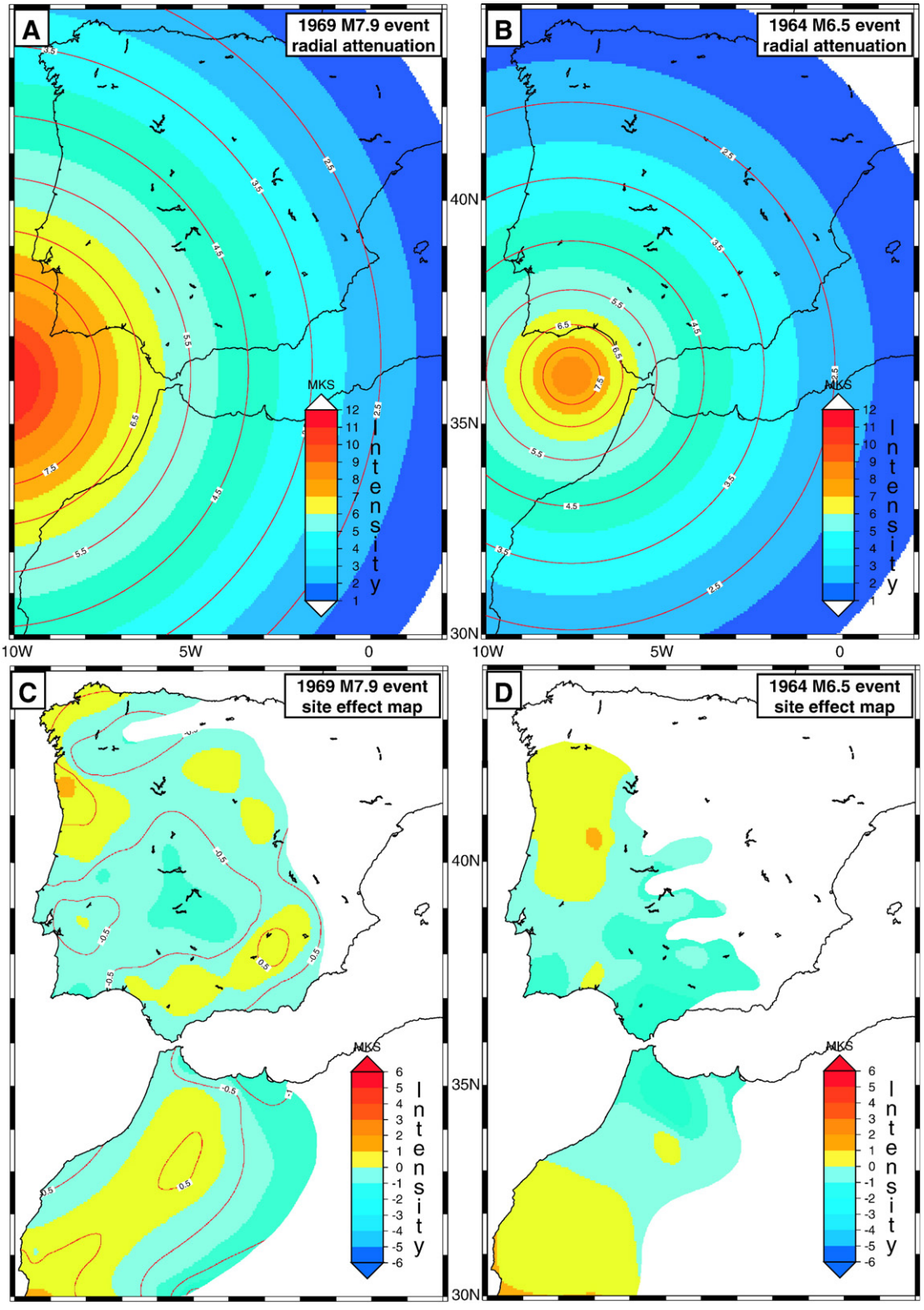

Fig. 6. Radial attenuation function for; A) M7.9 Cape St. Vincent earthquake of 1969, B) M6.8 Gulf of Cadiz earthquake of 1964. Calculated site effect maps for C) M7.9 Cape St. Vincent earthquake of 1969, D) M6.8 Gulf of Cadiz earthquake of 1964.

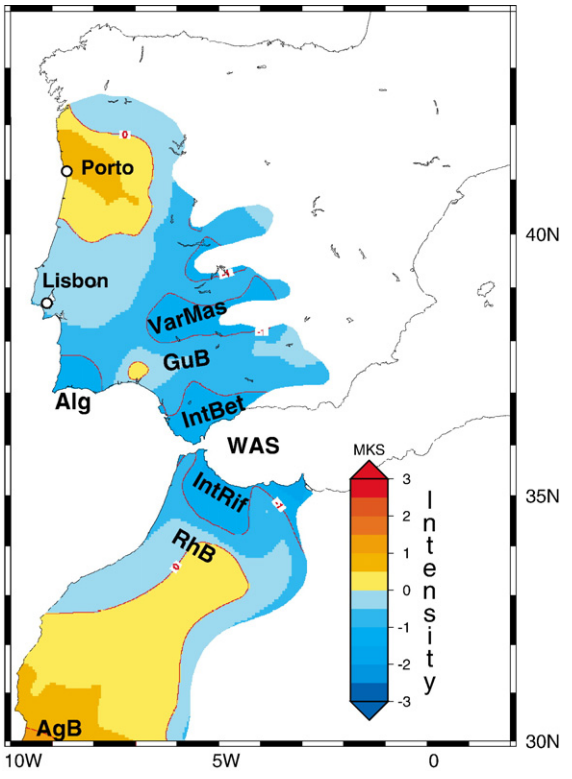

Fig. 7. Mean site-effect map using 1969 and 1964 earthquakes. Alg = Algarve, VarMas = Variscan Massifs, GuB = Guadalquivir Basin, IntBet = Internal Betic Zone, IntRif = Internal Rif Zone, WAS = West Alboran Sea, RhB = Rharb Basin, AgB = Agadir Basin.

tainties remain regarding reports of $I=8$ in Meknes, Fez and Marrakech and $I=7$ in Agadir. These historically observed values (Levret, 1991) are 1–2 intensities higher than predicted by such a source.

5. Discussion

Three other candidate sources have been proposed for the 1755 earthquake; Gorringe Bank, Marquis de Pombal and the Horseshoe fault (Fig. 1). Following the M7.9 St. Vincent earthquake in 1969, which occurred on the Horseshoe Fault in the Horseshoe abyssal plain, some authors proposed this to be the source of the 1755 earthquake as well (Fukao, 1973; Levret, 1991). The fault plane solution indicates conjugate N60° striking, 45° dipping fault planes with a reverse sense of motion. Other authors proposed the nearby Gorringe Bank, an uplifted flake of oceanic crust (rising to a water depth of 25 m), to be the source (Johnston, 1996). Seismic profiles reveal steep scarps and deformed sediments suggestive of recent thrust deformation here (Sartori et al., 1994; Hayward et al., 1999). The potential dimensions of a lithospheric scale thrust fault for Gorringe Bank are about 200 km × 80 km (for a 50 km thick elastic lithosphere, and 40° fault dip). Using a very high rigidity value of 6.5×10^{10} Pa (for a fault entirely in oceanic lithosphere), a magnitude of 8.7 was calculated for a uniform slip of 12 m (Johnston, 1996). For a more typical rigidity value of about 3×10^{10} Pa, a uniform slip of 24 m would be required to produce an M8.7 event.

More recently, authors have focussed on the Marquis de Pombal, a basement high off the SW corner of Portugal (Zitellini et al., 2001; Terrinha et al., 2002; Gracia et al., 2003). Tsunami modeling suggests a source located at the Marquis de Pombal structure can provide a reasonable fit for arrival time for most stations, though discrepancies exist for the Gulf of Cadiz and NW Moroccan coast (Baptista et al., 1998b). The primary objection to the Marquis de Pombal source, however, is that the dimensions of this structure (about 100 km × 70 km) are too modest to produce an earthquake of $M>8.5$. A calculation using a uniform slip of 15 m, yields only $M=8.3$ (Zitellini et al., 2001). An event of this magnitude would not be felt in Hamburg or the Cape Verde Islands. Indeed, an empirical relation has been established between fault rupture length and moment magnitude (Wells and Coppersmith, 1994). This relation suggests the dimensions of the source region of an M8.7 earthquake should be at least 200–300 km in length (Fig. 9). Of the known tectonic structures off SW Iberia, only Gorringe and the subduction fault plane have the necessary dimensions (200 km). The Marquis de Pombal is 70–100 km in size and is alone incapable of generating the appropriate seismic moment.

For these three previously proposed source regions, the tectonic shortening is considered to be the result of relative convergence along the Africa–Iberia plate boundary. Plate kinematic models estimate this motion to be about 4 mm/a (Argus et al., 1989; Fernandes et al., 2003). Thus, in order to accumulate 12, 15 or 24 m of total slip, a period of 3, 4 or 6 thousand years, respectively, would be necessary.

Therefore, one of the major questions to address, in the search for a candidate source, is what is the recurrence time of great earthquakes like the 1755 event? Two independent sets of sedimentological data provide clues as to this recurrence time, turbidites in the abyssal plains, and tsunami related overwash deposits in lagoons.

Sediment cores from the Horseshoe Abyssal Plain have sampled a series of turbidite deposits covering the entire abyssal plain with thicknesses ranging from 20 cm to over 2 m (Lebreiro et al., 1997). The volumes of several of these turbidite flows, exceeds 1 km^3. A maximum of 21 individual turbidites were cored spanning roughly the period since 35 ka (Lebreiro et al.,

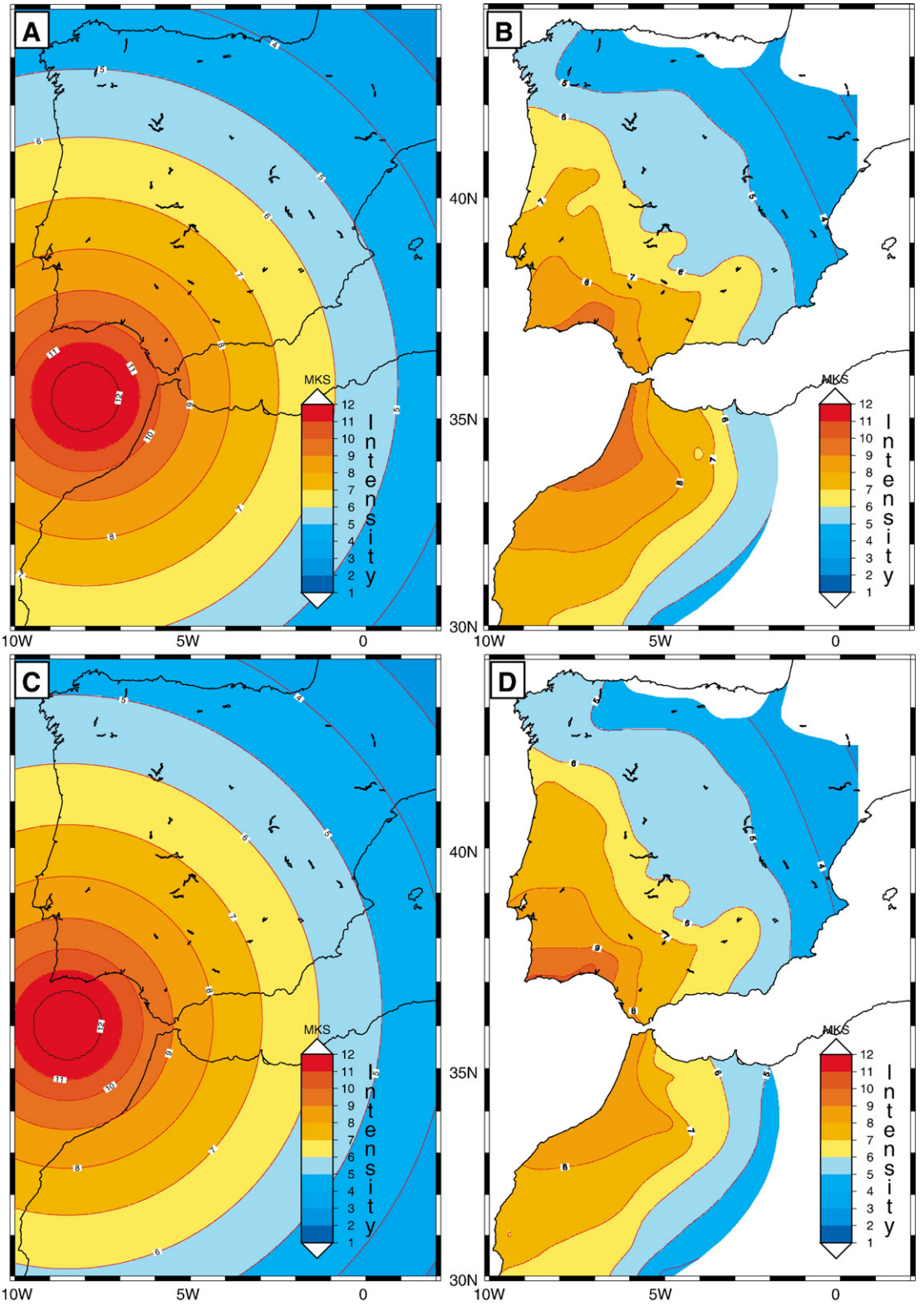

Fig. 8. Radial attenuation function and synthetic isoseimal maps, respectively, calculated for; A,B) a subduction fault plane source centered at 8° W, 35.5° N, C,D) a source at 8.5° W, 36° N, E,F) a source on the Marquis de Pombal, situated 100 km SW of Cape St. Vincent at 9.5° W, 36.5° N. In all cases there is zero attenuation (constant intensity I) within the source region.

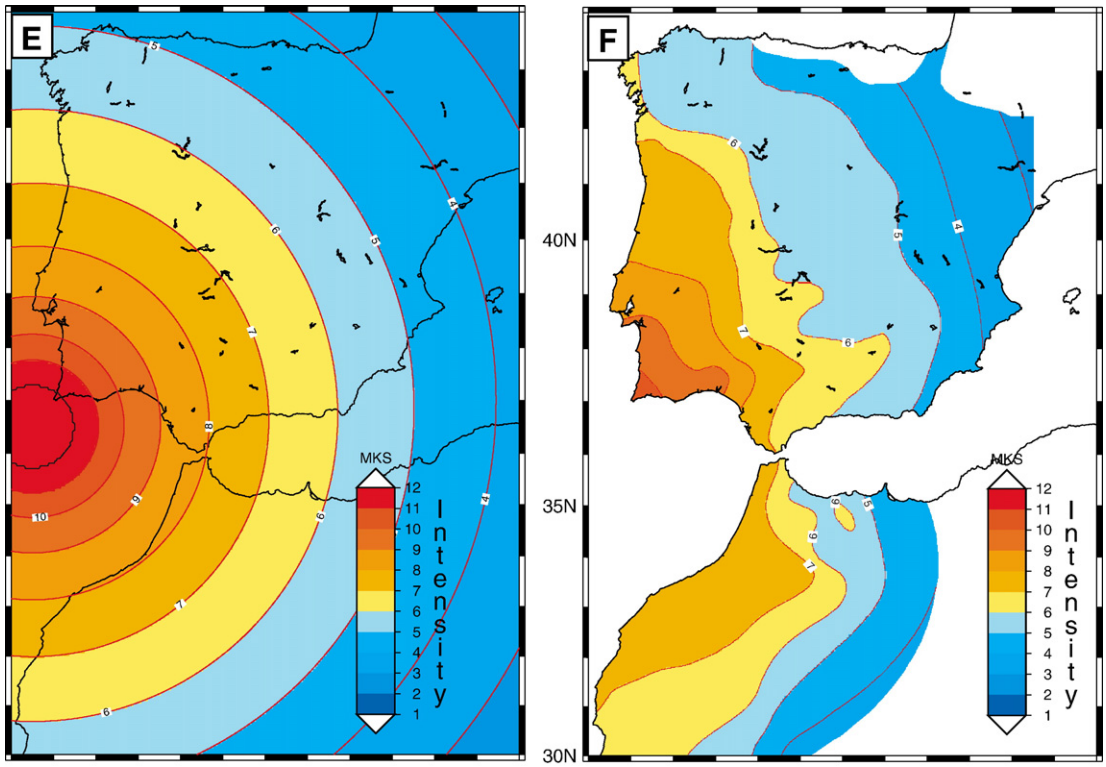

Fig. 8 (*continued*).

1997). The upper most turbidite in both the Horseshoe and Tagus abyssal plains has been dated as being contemporaneous with the 1755 earthquake (Thomson and Weaver, 1994). The older turbidites are likely to have been triggered by great earthquakes in the past. The chronology of these turbidite flows suggests a periodicity of 1000–2000 years.

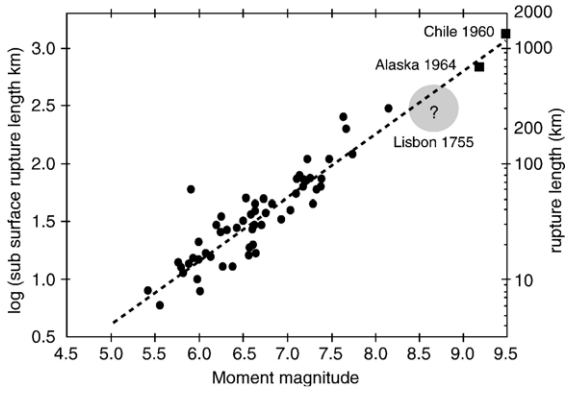

Fig. 9. Empirical relation between fault rupture length and earthquake moment magnitude (Wells and Coppersmith, 1994), with known values for 1964, M9.2 Alaska earthquake and 1960, M9.5 Chile earthquake and probable values for the 1755 Lisbon earthquake added.

Coarse-grained deposits in the lagoon behind a sandspit near Cadiz were identified as overwash deposits generated by a tsunami, because the 6 m high sand barrier is well above the maximum storm surge height. Dating allowed this tsunami deposit to be correlated to the 1755 earthquake. An older tsunami deposit beneath the first was dated at 2200 BP (200 BC) (Luque et al., 2001). If the source of these two tsunamis is the same, then a recurrence time on the order of 2000 years is indicated.

Thus, these two different types of sedimentological data both suggest a recurrence time on the order of 1000–2000 years. This recurrence time is generally consistent with the convergence rates indicated by GPS measurements in the Morocco–Iberia region, suggesting westward motion of stations in the Gibraltar block at velocities of 5–10 mm/a (Reilinger et al., 2001; Mourabit et al., 2002). For such velocities, 10–20 m of slip could accumulate during the inter-seismic phase of the seismic cycle along a locked fault zone.

6. Conclusions

The dimensions of the Gibraltar subduction fault plane (roughly 200×200 km) are sufficient to generate an earthquake of moment magnitude $M=8.80$ for a co-

seismic slip of 20 m or of $M=8.64$ for a co-seismic slip of 10 m. Tsunami modeling indicates general agreement with historical travel time and amplitude observations for about half the cities in the study area. A subduction source alone offers a better fit to the historical tsunami reports for stations in the Gulf of Cadiz–Morocco area than the Marquis de Pombal or other source further west (Baptista et al., 1998b). However, late arrivals and low amplitudes remain for the modeled tsunami along the Portuguese west coast and for Safi (Morocco). Macroseismic analysis suggests a source at the NW of the Gulf of Cadiz is best able to produce the historically observed seismic intensities and that a subduction fault plane alone may not be sufficient. But the subduction source appears likely to have contributed to the 1755 earthquake in generating the tremendous seismic moment, which no other tectonic structure in the region is large enough to produce alone. Also, the recurrence interval of great earthquakes in the region (1000–2000 years) is better explained by a slip along the subduction fault plane than other candidate sources discussed thus far. A combination of the subduction fault plane and an additional source further to the NW may offer the best explanation for the historically observed tsunami and seismic intensity patterns in the region. Historical reports of multiple (2–3) ground shaking events over the span of 10 min (Vilanova et al., 2003) support the notion of a complex multiple rupture. One possible scenario is that rupture of a ENE trending segment of the Africa–Iberia plate boundary in the Gorringe—Northern Gulf of Cadiz area, may have triggered rupture along the subduction fault plane.

Acknowledgments

We thank the French–Portuguese cooperation project for funding the travel between France and Portugal and the Portuguese MATESPRO project for organizing the Lisbon meeting which helped initiate this collaborative research project. We also thank the reviewers for their constructive suggestions. And we particularly thank L. Matias for the assistance in calculating the attenuation functions and determining the site effects for the study area. This article is a IUEM contribution 993.

References

Argus, D.F., Gordon, R.G., Demets, C., Stein, S., 1989. Closure of the Africa–Eurasia–North America plate motion circuit and tectonics of the Gloria fault. J. Geophys. Res. 94, 5585–5602.

Baptista, M.A., Heitor, S., Miranda, J.M., Miranda, P.M.A., Mendes Victor, L., 1998a. The 1755 Lisbon; evaluation of the tsunami parameters. J. Geodyn. 25, 143–157.

Baptista, M.A., Miranda, P.M.A., Miranda, J.M., Mendes Victor, L., 1998b. Constraints on the source of the 1755 Lisbon tsunami inferred from numerical modelling of historical data on the source of the 1755 Lisbon tsunami. J. Geodyn. 25, 159–174.

Baptista, M.A., Miranda, P.M.A., Chierici, F., Zitellini, N., 2003. New study of the 1755 earthquake source based on multi-channel seismic survey data and tsunami modeling. Nat. Hazards Earth Sci. Syst. 3, 333–340.

Buforn, E., Udias, A., Colombas, A., 1988. Seismicity, source mechanisms and tectonics of the Azores–Gibraltar plate boundary. Tectonophysics 356, 89–118.

Calvert, A., Sandvol, E., Seber, D., Barazangi, M., Roecker, S., Mourabit, T., Vidal, F., Alguacil, G., Jabour, N., 2000. Geodynamic evolution of the lithosphere and upper mantle beneath the Alboran region of the western Mediterranean: constraints from travel time tomography. J. Geophys. Res. 105, 10871–10898.

Chester, D.K., 2001. The 1755 Lisbon earthquake. Prog. Phys. Geogr. 25, 363–383.

Fernandes, R.M.S., Ambrosius, B.A.C., Noomen, R., Bastos, L., Wortel, M.J.R., Spakman, W., Govers, R., 2003. The relative motion between Africa and Eurasia as derived from ITRF2000 and GPS data. Geophys. Res. Lett. 30 (N.16), 1828, doi:10.1029/2003GL017089.

Fukao, Y., 1973. Thrust faulting at a lithospheric plate boundary: the Portugal earthquake of 1969. Earth Planet. Sci. Lett. 18, 205–216.

Gjevik, B., Pedersen, G., Dybesland, E., Harbitz, C.B., Miranda, P.M.A., Baptista, M.A., Mendes Victor, L., Heinrich, P., Roche, R., Guesmia, M., 1997. Modeling tsunamis from earthquake sources near Gorringe Bank southwest of Portugal. J. Geophys. Res. 102 (C13), 27931–27949.

Gracia, E., Danobeitia, J.J., Verges, J., PARSIFAL Team, 2003. Mapping active faults offshore Portugal (36°N–38°N): implications for seismic hazard assessment along the southwest Iberian margin. Geology 31, 83–86.

Gutscher, M.-A., Malod, J., Rehault, J.-P., Contrucci, I., Klingelhoefer, F., Mendes-Victor, L., Spakman, W., 2002. Evidence for active subduction beneath Gibraltar. Geology 30, 1071–1074.

Gutscher, M.-A., 2004. What caused the Great Lisbon earthquake? Science 305, 1247–1248.

Hayward, N., Watts, A.B., Westbrook, G.K., Collier, J.S., 1999. A seismic reflection and GLORIA study of compressional deformation in the Gorringe Bank region, eastern North Atlantic. Geophys. J. Int. 138, 831–850.

Holdahl, S.R., Sauber, J., 1994. Coseismic slip in the 1964 Prince William Sound earthquake: a new geodetic inversion. Pure Appl. Geophys. 142, 55–82.

Jimenez-Munt, I., Fernandez, M., Torne, M., Bird, P., 2001. The transition from linear to diffuse plate boundary in the Azores–Gibraltar region: results from a thin sheet model. Earth Planet. Sci. Lett. 192, 175–189.

Johnson, J.M., Satake, K., Holdahl, S.R., Sauber, J., 1996. The 1964 Prince William Sound earthquake: joint inversion of tsunami and geodetic data. J. Geophys. Res. 101, 14,965–14,991.

Johnston, A., 1996. Seismic moment assessment of earthquakes in stable continental regions — III. New Madrid, 1811–1812, Charleston 1886 and Lisbon 1755. Geophys. J. Int. 126, 314–344.

Lebreiro, S.M., McCave, I.N., Weaver, P., 1997. Late Quaternary turbidite emplacement on the horseshoe abyssal plain (Iberian margin). J. Sediment. Res. 67, 856–870.

Levret, A., 1991. The effects of the November 1, 1755 “Lisbon’’ earthquake in Morocco. Tectonophysics 193, 83–94.

Luque, L., Lario, J., Zazo, C., Goy, J.L., Dabrio, C.J., Silva, P.G., 2001. Tsunami deposits as paleoseismic indicators: examples from the Spanish coast. Acta Geol. Hisp. 36, 197–211.

Mader, C., 1988. Numerical modelling of water waves. Los Alamos Series in Basic and Applied Sciences. 206 pp.

Martinez-Solares, J.M., Lopez, A., Mezcua, J., 1979. Isoseismal map of the 1755 Lisbon earthquake obtained from Spanish data. Tectonophysics 53, 301–313.

Mendes Victor, L., Baptista, M.A., Miranda, J.M., Miranda, P.M.A., 1999. Can hydrodynamic modelling of tsunami contribute to seismic risk assessment? Phys. Chem. Earth 24, 139–144.

Mourabit, T., Ben Sari, D., Reilinger, R., McClusky, S., Gomez, F., Barazangi, M., 2002. Preliminary evidence of active deformation in Morocco from repeat GPS observations, Proceedings, Wegener 2002 Conference, June 2002, Athens, Greece (abstract).

Negredo, A., Bird, P., Sanz de Galdeano, C., Buforn, E., 2002. Neotectonic modeling of the Ibero–Maghrebian region. J. Geophys. Res. 107 (B11), 2292, doi:10.1029/2001JB000743.

Okada, Y., 1985. Surface deformation due to shear and tensile faults in a half-space. Bull. Seismol. Soc. Am. 75, 1135–1154.

Park, J.-O., Tsuru, T., Kodaira, S., Cummins, P.R., Kaneda, Y., 2002. Splay faults branching along the Nankai subduction zone. Science 297, 1157–1160.

Reilinger, R., McClusky, S., Ben Sari, D., Mourabit, T., Gomez, F., Barazangi, M., 2001. Active deformation in Morocco from repeat GPS observations, EOS Trans. AGU, Fall Meeting 2001 suppl., (abstract).

Sartori, R., Torelli, L., Zitellini, N., Peis, D., Lodolo, E., 1994. Eastern segment of the Azores–Gibraltar line (central-eastern Atlantic): an oceanic plate boundary with diffuse compressional deformation. Geology 22, 555–558.

Satake, K., Wang, K., Atwater, B.F., 2003. Fault slip and seismic moment of the 1700 Cascadia earthquake inferred from Japanese tsunami descriptions. J. Geophys. Res. 108 (B11), 2535, doi:10.1029/2003JB002521.

Smith, W.H.F., Sandwell, D.T., 1997. Global seafloor topography from satellite altimetry and ship depth soundings. Science 277, 1956–1962.

Terrinha, P., Pinheiro, L.M., Henriet, J.-P., Matia, L., Ivanov, A.K., Monteiro, J.H., Akhmetzhanov, A., Volkonskaya, Cunha, M.R., Shaskin, P., Rovere, M., 2002. Tsunamigenic–seismogenic structures, neotectonics, sedimentary processes and slope instability on the Southwest Portugese Margin. Mar. Geol. 195, 55–73.

Thiebot, E., Gutscher, M.-A., 2006. The Gibraltar Arc seismogenic zone (part 1): constraints on a shallow east dipping fault plane source for the 1755 Lisbon earthquake provided by seismic data, gravity and thermal modeling. Tectonophysics 246, 135–152 (this volume).

Thomson, J., Weaver, P., 1994. An AMS radiocarbon method to determine the emplacement time of recent deep-sea turbidites. Sediment. Geol. 89, 1–7.

Udias, A., Arroyo, A.L., 1970. Body and surface wave study of source parameters of the March 15, 1964 Spanish earthquake. Tectonophysics 9, 323–346.

Vilanova, S.P., Nunes, C.F., Foncesca, J.F.B.D., 2003. Lisbon 1755: a case of triggered onshore rupture? Bull. Seismol. Soc. Am. 93, 2056–2068.

Wells, D., Coppersmith, K., 1994. New empirical relationships among magnitude, rupture length, rupture width, rupture area and surface displacement. Bull. Seismol. Soc. Am. 84, 974–1002.

Zitellini, N., et al., 2001. Source of 1755 Lisbon earthquake and tsunami investigated. Eos (Transactions, American Geophysical Union) 82, 285–291.